Wrocław University of Environmental and Life Sciences

IAG GGOS
IGiG
TU WIEN
TECHNISCHE UNIVERSITÄT WIEN
Vienna University of Technology
GFZ
Helmholtz-Zentrum POTSDAM

Troposphere delay modeling in SLR solutions

Mateusz Drożdżewski[1], Krzysztof Sośnica[1], Janina Boisits[2], Kyriakos Balidakis[3] , Florian Zus[3], Dariusz Strugarek[1], Radosław Zajdel[1], Grzegorz Bury[1]

[1] Wroclaw University of Environmental and Life Sciences (Poland), Institute of Geodesy and Geoinformatics, [2] Vienna University of Technoldgy (Austria), [3] Helmholtz – Zentrum Potsdam – Deutsche GeoForschungsZentrum GFZ (Germany)

Motivation

Satellite Laser Ranging (SLR) is the only space geodetic technique in which troposphere models do not consider horizontal asymmetry of the atmosphere above the station. Due to low number of observations, poor geometry, and weather dependency the estimation of horizontal gradients from laser observation leads to a deterioration of weekly solutions. This work presents comparison of different approaches of troposphere delay modeling which are currently available.

PMF & VMF3o products

Differences between PMF, VMF3o and FCULa mapping functions projected onto elevation angles 10, 15 and 20 degrees are shown in figure 1. We observe characteristic differences between FCULa and PMF as well as VMF3o for stations located in the northern and southern hemisphere which reach more than 5 mm for 10 degrees elevation angles. For stations located in the northern hemisphere we also observe that the differences between solutions VMF3o and PMF could reach 1 mm.

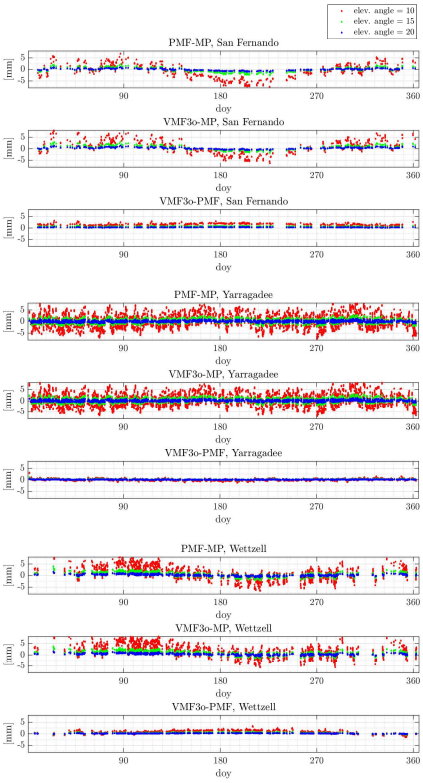

Fig 1.Impact of differences between PMF, VMF3o and FCULa mapping function projected onto 10, 15, 20 degrees elevation angle as a function of time.

Methodology

Function Commonly Used in Laser ranging (FCULa, Mendes et al., 2004):

$$m(e) = \frac{1+\frac{a_1}{1+\frac{a_2}{1+a_3}}}{sine+\frac{a_1}{sine+\frac{a_2}{sine+a_3}}}$$

$$d_{atm} = d^Z_{atm} \cdot m(e)$$

Vienna Mapping Function 3 optical (VMF3o Boisits et al., 2018):

$$m(e)_{VMF3oh} = \frac{1+\frac{a_h}{1+\frac{b_h}{1+c_h}}}{sine+\frac{a_h}{sine+\frac{b_h}{sine+c_h}}},$$

$$m(e)_{VMF3ow} = \frac{1+\frac{a_w}{1+\frac{b_w}{1+c_w}}}{sine+\frac{a_w}{sine+\frac{b_w}{sine+c_w}}}$$

$$d_{atm\,h} = d_h \cdot m(e)_{VMF3oh} + m_{gh}(G_{Nh} \cdot cosA + G_{Eh} \cdot sinA)$$

$$d_{atm\,w} = d_w \cdot m(e)_{VMF3ow} + m_{gw}(G_{Nw} \cdot cosA + G_{Ew} \cdot sinA)$$

$$d_{atm} = (d_{atm\,h} + d_{atm\,w})$$

Potsdam Mapping Function
(PMF, Zus F. et al., 2014, Drożdżewski et al., 2019) :

$$m(e)_{PMF} = \frac{1+\frac{a_1}{1+\frac{b_2}{1+c_3}}}{sine+\frac{a_1}{sine+\frac{b_2}{sine+c_2}}},$$

$$d_{atm} = d^Z_{atm} \cdot m_{PMF}(e) + (G_N \cos A + G_E \sin A) \cdot m_g(e)$$

$$d_{atm} = d^Z_{atm} \cdot m_{PMF}(e) + (G_N \cos A + G_E \sin A + G_{NN} \cos^2 A + G_{NE} \cos A * sinA + G_{EE} \sin^2 A) \cdot m_g(e)$$

FCULa + simple model of gradients derived from numerical wheather models (NWM):

$$f(t) = a_0 + a_1 t + a_{s1} \sin\left(\frac{2\pi}{T}t\right) + a_{c1} cos\left(\frac{2\pi}{T}t\right) + a_{s2} \sin\left(\frac{4\pi}{T}t\right) + a_{c2} cos\left(\frac{4\pi}{T}t\right)$$

Offset + drift + annual signal + semi-annual signal for each component for each SLR station
The example of model present figure 3.

$m(e)$ – mapping function,
e – elevation angle of observation
a_1, b_2, c_3 – common mapping function coefficients for hydrostatic and non – hydrostatic part of zenith delay.
a_h, b_h, c_h - hydrostatic mapping function coefficients
a_w b_w c_w - non – hydrostatic mapping function coefficients
d^Z_{atm}, d_h, d_w - The total zenith delay, the hydrostatic part of zenith delay, the non-hydrostatic part of zenith delay
m_g - Chen and Herring mapping function for horizontal gradients
G_N, G_E - The north and the east component of horizontla gradients

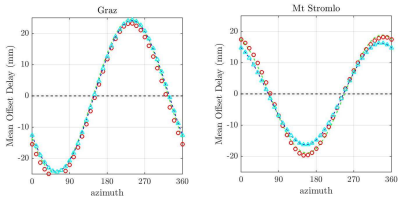

Fig. 2. Horizontal gradients derived from PMF (red circles) and VMF3o (blue triangles) projected onto 10 degrees elevation angle. The green dashed line describes the hydrostatic part of VMF3o.

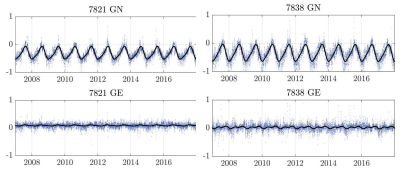

Fig. 3. Time series of troposphere delay horizontal gradients (PMF+ O1) with semi annual and annual signal (black line).

Observation residuals

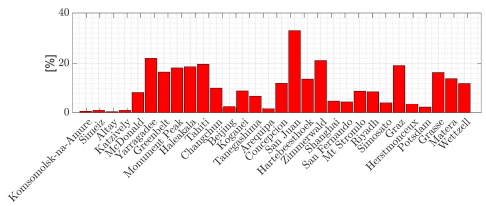

Fig 4. Percentage of observations below 27 degrees of elevation angle. Analyzed period 2007.0 – 2010.0.

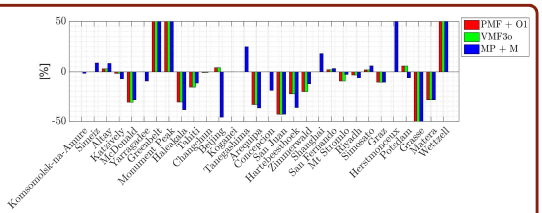

Fig 5. Differences of median value of residuals for observations provided below 27 degree of elevation angle. Analyzed period 2007.0 – 2010.0.

In analysed period observations below 27 degrees constitute on average 10 % of total amount of observations. For station San Juan this value reaches over 32%. For the majority of the stations, observations provided at low elevation angle constitute above 15% of all observations to LAGEOS-1 and LAGEOS-2.

The negative values correspond to a reduction of mean biases (median residuals) for solutions based on PMF, VMF3o or FCULa + model with respect to the standard aproach. Nevertheles for some stations we observe a significant deterioration of observation resiudals (Greenbelt, Monument Peak and Wetzell).

Earth rotation parameters

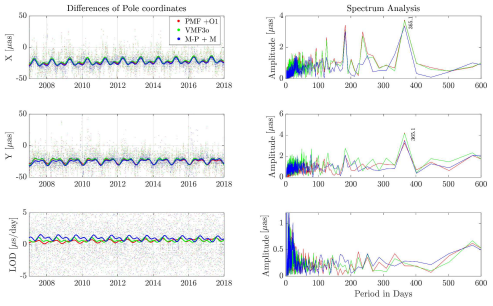

Fig 6. Differences of Earth rotation parameters, between the standard solution and solutions with Horizontal gradients. The continuous bold lines present the annual and semi-annual signals fitted into timeseries.

Tab. 1 Differences between estimated Earth rotation parameters and the IERS-C04-14.

	X-POLE (μas)		Y-POLE (μas)		LOD (μs/day)		Number of epochs
	OFF	SIG	OFF	SIG	OFF	SIG	
Standard sol.	22	7.5	38	7.6	-77	5.2	574
PMF + O1	2	7.5	14	7.6	-77	5.2	574
VMF3o	10	7.5	12	7.6	-76	5.2	574
M-P + M	7	7.5	11	7.6	-75	5.2	574

Geocenter coordinates

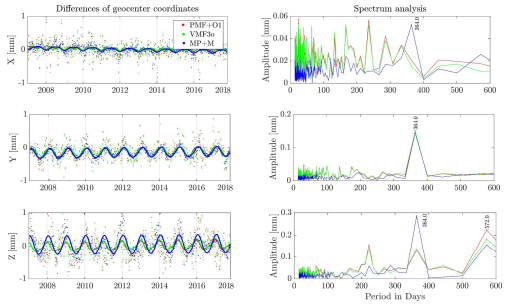

Fig 7. Differences of geocenter coordinates between the standard solution and solutions with horizontal gradients.

Figure 6 show differences between pole coordinates including PMFs, VMF3o models and the standard FCULa approach. The solutions with horizontal gradients are characterized by offsets at the range from 20 μas to 10 μas. We do not observe significant differences for LOD.
The consistency of the pole coordinates between SLR solutions with horizontal gradients and the IERS-14-C04 series is improved (for details see table below).

Conclusions

- In this study, we compared three solutions that consider azimuthal asymmetry of atmosphere above the stations with respect to currently used troposphere delay model. We observe that mapping functions projected at an elevation angle of 10 degrees show a significant difference.
- The differences of median values of observation residuals show an improvement at the level of 50% for low elevation angles for the station Grasse. These observations constitute 12% of the total amount of observations at the site.
- All models improved the consistency between pole coordinates derived from SLR and IERS-14-C04 combined series. Due to this fact, we recommend models that take account horizontal gradients.

References:
Drożdżewski M., Sośnica K., Zus F., Balidakis K. (2019)
Troposphere delay modeling with horizontal gradients for satellite laser ranging
Journal of Geodesy, Vol. online No. in print, Berlin- Heidelberg, Germany 2019, pp. 1-14
DOI: 10.1007/s00190-019-01287-1
URL: https://link.springer.com/article/10.1007/s00190-019-01287-1

Boisits J., Landskron D., Sośnica K., Drożdżewski M., Böhm J.
VMF3o: Enhanced Troposphere Mapping Functions for Optical Frequencies
21st International Workshop on Laser Ranging, Canberra, Australia, 4-9 November 2018 (proceedings), pp. 1-15
URL: https://cddis.nasa.gov/lw21/docs/2018/presentations/Session2_Boisits_presentation.pdf

Mendes V. B, Prates G, Pavlis E. C, Pavlis D. E, Langley R. B., n.d. (2002)
Improved mapping functions for atmospheric refraction correction in SLR.
Geophysical Research Letters 29, 53-1-53-4. https://doi.org/10.1029/2001GL014394

Zus F, Dick G, Douša J, Heise S,Wickert J (2014) **The rapid and precise computation of GPS slant total delays and mapping factors utilizing a numerical weather model.** Radio Sci 49(3):207–216. https:// 884
doi.org/10.1002/2013RS005280

VMF3o Products you can find here:
PMF Products you can find here:

Wrocław University of Environmental and Life Sciences